Composites: Part A 42 (2011) 2036–2042

Contents lists available at SciVerse ScienceDirect

Composites: Part A

journal homepage: www.elsevier.com/locate/compositesa

Hybrid multi-scale epoxy composite made of conventional carbon fiber fabrics with interlaminar regions containing electrospun carbon nanofiber mats

Qi Chen [a], Lifeng Zhang [a], Arifur Rahman [b], Zhengping Zhou [b], Xiang-Fa Wu [b,*], Hao Fong [a,*]

[a] Department of Chemistry, South Dakota School of Mines and Technology, Rapid City, SD 57701, USA
[b] Department of Mechanical Engineering, North Dakota State University, Fargo, ND 58108, USA

ARTICLE INFO

Article history:
Received 30 April 2011
Received in revised form 6 September 2011
Accepted 7 September 2011
Available online 13 September 2011

Keywords:
A. Polymer-matrix composites (PMCs)
A. Fibers
B. Mechanical properties
B. Electrical properties

ABSTRACT

Herein we report the development and evaluation of hybrid multi-scale epoxy composite made of conventional carbon fiber fabrics with interlaminar regions containing mats of electrospun carbon nanofibers (ECNs). The results indicated that (1) the interlaminar shear strength and flexural properties of hybrid multi-scale composite were substantially higher than those of control/comparison composite without ECNs; in particular, the interlaminar shear strength was higher by ~86%; and (2) the electrical conductivities in both in-plane and out-of-plane directions were enhanced through incorporation of ECNs, while the enhancement of out-of-plane conductivity (~150%) was much larger than that of in-plane conductivity (~20%). To validate the data reduction procedure, a new shear stress formula was formulated for composite laminates, which took into account the effect of layup and inter-layers. The study suggested that ECNs could be utilized for the development of high-performance composites, particularly with the improved out-of-plan properties (*e.g.*, interlaminar shear strength).

1. Introduction

Due to high specific strength and toughness, superior manufacturability, as well as excellent corrosion resistance and fatigue tolerance, composites made of polymeric resins reinforced with high-performance fibers (*e.g.*, carbon fibers) have a wide range of applications in aeronautical and astronautical structures (*e.g.*, aircraft, space shuttle, and satellite), ground vehicles, and sports utilities (*e.g.*, golf clubs and tennis/badminton racquets) [1]. In general, the composites are fabricated through impregnation of fibers (with high strength and modulus) into resin matrices; in practice, prepregs consisting of unidirectional or woven fiber fabrics are usually prepared prior to fabrication of the composites [2]. For laminated composites made of prepregs, the fiber fabrics dominate the in-plane mechanical properties that are typically high enough for applications, whereas the resin matrices dominate the out-of-plane mechanical properties (*e.g.*, interlaminar shear strength and delamination toughness) that are significantly lower than the in-plane properties [3]. To mitigate the problem, additional reinforcement agents have been incorporated (particularly between neighboring laminas within the composites) for the purpose of improving the out-of-plane properties [2,4]. In the recent decade, carbonaceous nanomaterials (*e.g.*, carbon nanotubes/nanofibers, exfoliated graphite nano-platelets, activated carbon, etc.) have attracted growing attentions as innovative reinforcement agents due to their capabilities of considerably improving out-of-plane properties for the resulting composites [5–16]. It has been predicted in theory and validated in benchmark experiments that the composites with uniformly distributed nano-reinforcement agents between neighboring laminas would possess superior mechanical properties [12–14]. To date, substantial research endeavors have been devoted to the exploration of processing methods that could result in uniform distribution of nano-reinforcement agents between the laminas of composites [15–17].

The materials-processing technique of electrospinning provides a straightforward and viable approach for convenient fabrication of fibers with diameters ranging from nanometers to microns [18,19]. Electrospun carbon nanofibers (ECNs) can be developed through thermal treatments (*i.e.*, stabilization followed by carbonization) of their electrospun precursors such as polyacrylonitrile (PAN) nanofibers. Our previous study indicated that the ECNs were capable of possessing superior mechanical properties (particularly the tensile strength) that would unlikely be achieved through conventional approaches [20]. This is primarily due to the following two reasons: (1) the innovative precursor, with fiber diameters being ~100 times smaller than that of conventional counterparts, would possess the high degree of macromolecular orientation and the substantially reduced amount of defects; and (2) the ultrathin diameters of fibers would also effectively prevent the formation of structural inhomogeneity (particularly sheath-core structures) during the thermal treatments [20].

* Corresponding authors. Tel.: +1 701 231 8836; fax: +1 701 231 8913 (X. Wu), tel.: +1 605 394 1229; fax: +1 605 394 1232 (H. Fong).
E-mail addresses: Xiangfa.Wu@ndsu.edu (X.-F. Wu), Hao.Fong@sdsmt.edu (H. Fong).

1359-835X/$ - see front matter © 2011 Elsevier Ltd. All rights reserved.
doi:10.1016/j.compositesa.2011.09.010

To the best of our knowledge, only limited research efforts have been carried out to develop and evaluate composites reinforced with electrospun nanofibers [14,21–24]. In this study, the ECN mats were prepared through electrospinning followed by stabilization and carbonization; the mats were then utilized as the nanoscale reinforcement for developing the hybrid multi-scale composite. As compared to the reported research activities on nanoscale reinforcement [2,3,5], the uniqueness and advantages of ECN mats include: (1) the mats can be readily sandwiched between conventional fabrics, thus the addition of ECNs does not result in substantial increase of processing cost; (2) since ECN mats are very thin, the addition of ECNs does not lead to significant weight increase of composite; and (3) since ECNs in the mats are randomly oriented, the distribution of ECNs between neighboring laminas in the composites are quite uniform. It is noteworthy that, unlike carbon nanotubes/nanofibers in the "bucky paper" and "nano paper" that are made through bottom-up synthetic methods, the ECNs are made through a top-down nano-manufacturing process; therefore, ECNs (and/or ECN mats) are cost-effective and can be readily sandwiched between conventional carbon fiber fabrics without substantial increase of processing cost. During this study, the SC-15 epoxy resin was selected as the polymeric matrix; a low-cost composite-manufacturing technique (*i.e.*, the vacuum assisted resin transfer molding (VARTM) method) was adopted for fabrication of composites. To investigate the effects of ECNs on the hybrid multi-scale composite, mechanical and electrical properties of the composite were evaluated. Specifically, the short-beam shear test and three-point flexural test were carried out to determine the interlaminar shear strength and flexural properties, respectively; while the measurements of electrical conductivity were conducted in both in-plane and out-of-plane directions. Scanning electron microscopy (SEM) was employed to examine the micro- and/or nano-scaled morphologies, the distribution of ECNs in the composites (particularly between neighboring laminas), and the fracture surfaces. Additionally, a new shear stress formula was formulated by taking into account the effects of ply layup and inter-layers. In the reduced case, the formula could cover the classic shear stress formula used for short-beam tests. Discussions on reinforcement mechanisms and conclusions of the study were made consequently.

2. Experimental

2.1. Materials

The epoxy resin of SC-15A and the hardener of SC-15B were supplied by the Applied Poleramic Inc. (Benicia, CA). Polyacrylonitrile (PAN) microfibers (SAF 3 K fibers) were provided by the Courtaulds Co. (Essex, UK). Acetone and *N,N*-dimethylformamide (DMF) were purchased from the Sigma–Aldrich Co. (St. Louis, MO). The woven fabrics of T300® carbon fibers were produced by the Toray Industries, Inc. (Tokyo, Japan).

2.2. Preparation of electrospun carbon nanofiber (ECN) mats

ECNs were prepared through electrospinning of PAN nanofibers followed by thermal treatments of stabilization and carbonization. Prior to electrospinning, the SAF 3 K microfibers were first immersed in acetone to remove the surface oil and then dissolved in DMF to prepare a 14 wt.% solution. Subsequently, the solution was filled in a 30-ml BD Luer-Lok™ plastic syringe installed with a stainless-steel needle having an 18-gauge 90° blunt end. The setup for electrospinning included a high voltage power supply (model number: ES30P), purchased from the Gamma High Voltage Research, Inc. (Ormond Beach, FL), and a laboratory-produced aluminum roller with diameter of 25 cm. During electrospinning, a DC voltage of 25 kV was applied between the needle and the grounded nanofiber collector; a flow rate of 1.0 ml/h was maintained by a syringe pump (model number: KDS 200) purchased from the KD Scientific Inc. (Holliston, MA). The PAN nanofibers were collected on aluminum foil (which was covered on the electrically grounded roller) as the mat consisting of randomly overlaid nanofibers. The angular velocity of the roller during electrospinning was set at 100 rpm. The collected PAN nanofiber mat had a width of ~10 cm, a thickness of ~40 μm, and a mass per unit area of ~15 g/m^2, and the nanofiber mat could be easily peeled from the aluminum foil after being immersed in ethanol. The stabilization and carbonization were conducted in a Lindberg 54,453 Tube Furnace purchased from the TPS Co. (Watertown, WI). During the stabilization, a constant flow of air was maintained through the furnace; the PAN nanofiber mats with the length of 3 in. and the width of 2 in. were sandwiched between two graphite plates and heated to 280 °C at a heating rate of 1 °C/min, the temperature was then held at 280 °C for 6 h. The stabilized mats were subsequently heated at a rate of 5 °C/min to 1200 °C in argon followed by holding the temperature at 1200 °C for 1 h to prepare the ECN fabrics.

2.3. Fabrication of hybrid multi-scale composite

The hybrid multi-scale composite (consisting of both T300® carbon fiber (CF) fabrics and the sandwiched ECN mats in the resin matrix of epoxy) were fabricated by the method of VARTM, as illustrated in Fig. 1. The mass ratio of a CF fabric versus an ECN mat (with the same length and width) was ~20. The mass ratio of the epoxy resin versus the hardener was set at 100:30. During the process, six layers of CF fabrics and five layers of ECN mats (with the length and width of 3 and 2 in. respectively) were used; the vacuum of 27 mm Hg was maintained during the initial curing at room temperature for 24 h. The obtained composite was further cured in an oven at 110 °C for 5 h before being characterized and evaluated. For comparison, the (conventional) composite with six CF fabrics alone was also fabricated and evaluated as the control/comparison sample.

2.4. Characterization and evaluation

A Zeiss Supra 40 VP field-emission scanning electron microscope (SEM) was employed to examine the morphologies of fibers as well as the fracture surfaces of composites. Prior to SEM examinations, the specimens were sputter-coated with gold to avoid charge accumulations.

Mechanical properties of the fabricated composites were tested at room temperature. The specimens for the flexural and short-beam shear tests were prepared and evaluated in accordance with ASTM D790 and ASTM D2344, respectively. The flexural specimens (50.8 mm in length, 12.7 mm in width, and 1.6 mm in thickness) and short-beam specimens (8 mm in length, 4 mm in width, and 1.6 mm in thickness) were cut from the fabricated composite panels by using a water-cooled diamond saw. The three-point flexural test with a support span of 25.4 mm was used to fracture the specimens on a QTESTTM/10 mechanical testing machine purchased from the MTS Systems Co. (Eden Prairie, MN). The constant strain rate (0.01 mm/mm/min) was maintained in the test. The short-beam shear test was carried out on specimens with span-to-thickness ratio of 4, and a cross-head speed of 1 mm/min was maintained until the failure of the specimen. Five specimens cut from each composite panel were tested, and the mean values and standard deviations of mechanical properties were calculated.

Electrical conductivities in both in-plane and out-of-plane directions of the composites were measured by using a Keithley

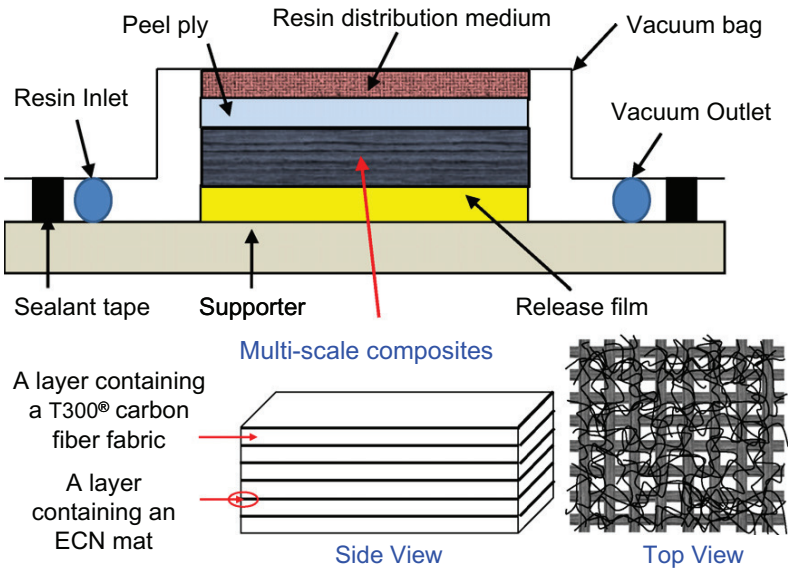

Fig. 1. Schematic illustration of the VARTM process and the hybrid multi-scale composite made of six layers of T300® CF fabrics and five layers of ECN mats. (For interpretation of the references to color in this figure legend, the reader is referred to the web version of this article.)

2612 system source meter. The specimens had the length, width, and thickness of 30 mm, 10 mm, and 1.2 mm, respectively. Prior to measurements, the surface of the specimens was polished to ensure a good contact with the silver paint electrodes. The measurements were performed on three specimens made from each type of composites.

3. Results and discussion

3.1. Mechanical properties

3.1.1. Interlaminar shear strength

The short-beam shear test was carried out to measure the interlaminar shear strength of the fabricated composites. Interlaminar shear strength is to describe the composite's resistance against the interlaminar shear failure such as commonly observed free-edge delamination in angle-ply polymer composites. For short-beam shear test, the shear strength of a specimen can be determined using the following formula:

$$\tau_s = 0.75\frac{P_m}{b \times h}, \quad (1)$$

where τ_s is the shear strength of the specimen (MPa), P_m is the peak load recorded in the test (N), b is the specimen width (mm), and h is the specimen thickness (mm).

Fig. 2A shows two typical load–displacement curves acquired experimentally from the composites with and without ECNs, respectively. It is evident that the incorporation of ECNs substantially increases the flexural rigidity (stiffness) and failure load. The values of interlaminar shear strength and the corresponding standard deviations for the tested composites are shown in Table 1. For comparison, two types of composites were evaluated: the one made of six layers of T300® CF fabrics in the epoxy resin without ECN mats, and the other made of six layers of CF fabrics sandwiched with five layers of ECN mats. Each datum in the table provides the mean value of five measurements with the corresponding standard deviation. The results indicated that the hybrid multi-scale composite with interlaminar regions containing ECNs possessed substantially higher interlaminar shear strength than the control composite without ECNs. The experimental values of interlaminar shear strength for the composites with and without ECN reinforcement were (51.2 ± 4.9) MPa and (27.5 ± 1.3) MPa, respectively. Thus, the interlaminar shear strength was improved by ~86% after the incorporation of ECNs. The interlaminar regions in conventional composites reinforced with carbon fiber fabrics are weak due to presence of neat resin layers between neighboring plies and lack of transverse reinforcement; in contrast, the incorporation of ECNs considerably strengthens the interlaminar regions in the resulting hybrid multi-scale composite. In this case, the ECNs act as nano-reinforcement in these interlaminar regions. It is noteworthy that the entanglement of ECNs could effectively mitigate the propagation of micro-cracks in the resin-rich interlaminar regions. Phenomenologically, if a micro-crack initiates in the regions due to stress concentration, the ECNs remain intact across the crack plane and support the applied load similar to the hooks and loops in Velcro [13]. Hence, the crack propagation can be effectively suppressed by the bridging nanofibers; consequently, the epoxy matrix is reinforced.

3.1.2. Flexural properties

Fig. 2B shows two typical experimental load–deflection curves of three-point bending tests for the composites with and without ECNs, respectively. Similar to the ones shown in Fig. 2A, the composite with ECNs had much higher stiffness and failure load. Based on the experimental load–deflection curves, the flexural strength (FS), flexural modulus (FM), and work of fracture (WOF) of the composites can be extracted (see Table 1). The results indicated that the FS, FM, and WOF were all increased upon impregnation of ECN mats into the composites. The values of FS, FM, and WOF for the CF-epoxy composite (without ECN mats) are (376.9 ± 11.8) MPa, (30.1 ± 1.0) GPa, and (11.2 ± 0.5) kJ/m^2, respectively; while those for the hybrid multi-scale CF/ECN-epoxy composite are (418.5 ± 11.7) MPa, (32.8 ± 7.8) GPa and (13.6 ± 0.6) kJ/m^2, respectively. The improvements of FS, FM, and WOF resulted from incorporation of ECN mats are 11.1%, 9.3%, and 21.4%, respectively. In general, mechanical properties of fiber-reinforced polymer composites are dominated by the mechanical properties and volume fraction of the reinforcing fibers. The impregnation of ECNs into the interlaminar regions led to the increase of flexural properties for the resulting CF/ECN-epoxy composite. The ECNs (with

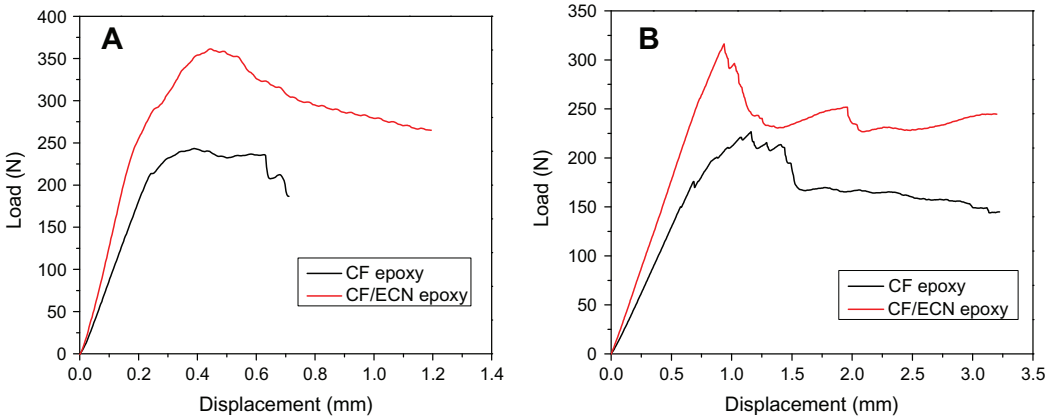

Fig. 2. Typical load–displacement curves recorded from the short-beam shear test (A) and three-point flexural test (B) of the CF-epoxy and CF/ECN-epoxy composites. (For interpretation of the references to color in this figure legend, the reader is referred to the web version of this article.)

Table 1
Mechanical properties of (conventional) CF-epoxy composite and (hybrid multi-scale) CF/ECN-epoxy composite. Each datum shows the mean value of five measurements and the corresponding one standard deviation.

Composites	Interlaminar shear strength (MPa)	Flexural properties		
		Strength (MPa)	Modulus (GPa)	Work of fracture (kJ/m^2)
CF-epoxy	27.5 ± 1.3	376.9 ± 11.8	30.1 ± 1.0	11.2 ± 0.5
CF/ECN-epoxy	51.2 ± 4.9	418.5 ± 11.7	32.8 ± 7.8	13.6 ± 0.6

diameters much smaller than those of the T300® CFs) could strongly bond to the epoxy resin due to much higher specific surface area, resulting in the improvement of interfacial bonding strength; consequently, the flexural strength of the CF/ECN-epoxy composite could be improved. Additionally, ECNs could also be broken and/or detached from the matrix of epoxy resin when the load is applied; this would dissipate the strain energy, preventing the failure of the composite and leading to the higher value of work of fracture.

3.2. Fiber morphology, fracture surface, and reinforcement mechanism

SEM images in Fig. 3 show the representative morphologies of (A) T300® CF fabric (with the inset showing the microfiber architecture in the fabric) and (B) ECN mats, as well as the typical fracture surfaces (in the interlaminar region) of the CF-epoxy composite (C) and CF/ECN-epoxy composite (D). The diameter of ECNs was ~0.7 μm; in contrast, the diameter of T300® CFs was ~7 μm. It is noteworthy that, during the typical interlaminar short-beam shear and three-point flexural tests of the laminated composites, the shear stress is transferred from ply to ply through the resin matrix. Thus, delamination is one of the primary failure mode responsible for interfacial failure; while other failure modes (such as resin matrix cracking and fiber pull-out and debonding) may also contribute to the failure [25,26]. Generally speaking, to mitigate the delamination of laminated composites, mechanical properties of both the resin matrix and the fiber/matrix interface have to be improved. Since the ECNs are one order of magnitude thinner than the T300® CFs, the specific surface area of ECNs is one order of magnitude larger than that of the T300® CFs. Hence, the interface of ECN/epoxy is expected to be much stronger than that of CF/epoxy.

It was observed that the deformation and fracture usually occurred in the interlaminar regions for both CF-epoxy and CF/ECN-epoxy composites, as shown in Fig. 3C and D. For the CF-epoxy composite, the fracture surface was relatively smooth with oriented fracture features; these features were resulted from the extensions of micro-cracks initiated at the locations of stress concentration. In contrast, the fracture surface of the CF/ECN-epoxy composite was much rougher without clearly identifiable fracture lines. These results indicated that the presence of ECNs could deflect the micro-cracks, and thus increase the resistance to propagation of cracks. When the cracks finally broke away from the fibers, kinked fracture surfaces were created, suggesting more strain energy dissipation during cracking. Voids/holes were also detected on the crack surfaces of the CF/ECN-epoxy composite due to pull-out and debonding of ECNs. This indicated that the interfacial bonding strength can be further improved, for example, through surface treatment of ECNs. On the other hand, the ECN debonding failure may also positively contribute to the high fracture toughness of the composite.

3.3. Electrical conductivity

In this study, both in-plane and out-of-plane electrical conductivities were measured for the CF/ECN-epoxy and CF-epoxy composites. The (in-plane) electrical conductivity of ECN mats was also determined using the same characterization method as-described in the experimental section, and the value was in the range of 600–700 S/cm. As shown in Fig. 4, the CF/ECN-epoxy composite demonstrated higher electrical conductivities compared to those of the CF-epoxy composites. The average value of in-plane electrical conductivity for the CF/ECN-epoxy composite was 175.67 S/cm, ~20% higher than that of the CF-epoxy composite. Since both T300® CFs and ECNs are electrically conductive, the addition of ECNs would improve the electrical conductively in the in-plane direction. Results in Fig. 4 also show that the electrical conductivities in out-of-plane direction were approximately three to four orders of magnitude lower than those in in-plane direction for both types of composites. This is due to the interlaminar regions enriched with electrically non-conductive epoxy resins [17]. The out-of-plane conductivity of CF/ECN-epoxy composite, however, was 0.0393 S/cm, which was ~150% higher than that of CF-epoxy composite. It is noteworthy that the T300® CFs were highly

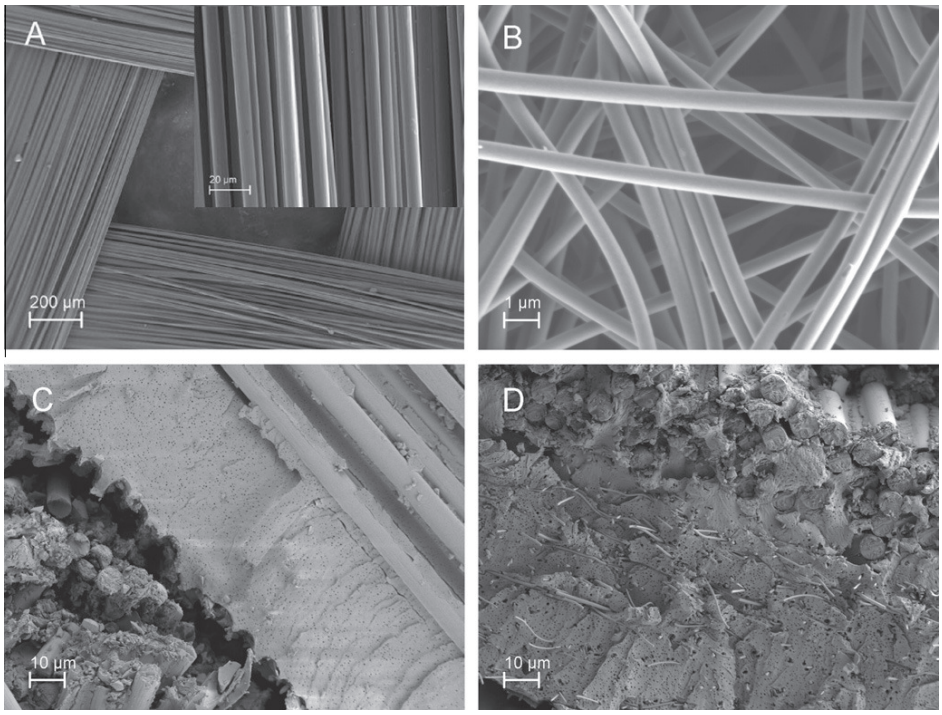

Fig. 3. SEM images showing the representative morphologies of (A) T300® CF fabric (with the inset showing a microfiber bundle in the fabric) and (B) ECN mat, as well as the typical fracture surface (in the interlaminar region) of CF-epoxy composite (C) and CF/ECN-epoxy composite (D).

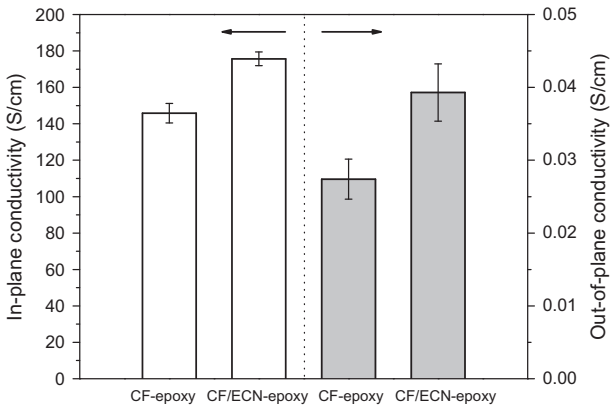

Fig. 4. The in-plane conductivity (left panel) and out-of-plane conductivity (right panel) of the fabricated CF-epoxy and CF/ECN-epoxy composites. Each datum is the mean value of three measurements with error bar representing one standard deviation.

oriented, while the ECNs were randomly distributed; thus, the improvement of out-of-plane conductivity for the CF/ECN-epoxy composite was much higher than the improvement of in-plane conductivity. The electrical conductivity of the fabricated composite containing ECNs is comparable to that of the composite containing carbon nanotubes/nanofibers [2].

3.4. Effect of laminate configuration on experimental characterization of interlaminar shear strength

In this study, the experimental values of interlaminar shear strength were extracted using Eq. (1). Although this equation has been widely adopted by many researchers to extract the interlaminar shear strength values of composite materials [27], it needs to be cautious to use the equation for laminated composites, since it does not take into account the stacking sequence of the laminates and the formula is based on the classic beam theory (slender beams). Herein, we modify the former part within the framework of slender composite beam theory as a good approach for experimental data reduction of composite laminates.

For cross-ply laminated composites which can be treated as being made of orthotropic laminas, a modified shear strength formula for data reduction can be formulated using mechanics of composite materials [28–30]. For an ECN/CF-epoxy (laminated) composite made of n layers of CF fabrics (effectively isotropic), n is an even number for the purpose of shear strength test, the effective modulus, Poisson's ratio, and thickness of the composite laminas (excluding the ultrathin interlaminar resin layers) after curing are denoted as E_c, υ_c, and t_c, respectively. The number of the ECN mat layers (effectively isotropic) is $n-1$, and the corresponding effective modulus, Poisson's ratio, and thickness of the ECN layers are E_n, υ_n, and t_n, respectively. Based on the composite beam theory [28–30] and the short-beam shear test configuration, the maximum shear stress (shear strength) at the mid-plane (as shown in Fig. 5) can be expressed as:

$$\tau_s = \frac{Q_{comp} P_m/2}{b(\Sigma EI)}. \tag{2}$$

In Eq. (2), P_m is the maximum load at the shear failure point; Q_{comp} is the first moment of the effective modulus of the upper half cross-section of the laminate (*i.e.*, the cross-section with $z \geqslant 0$), defined as:

$$Q_{comp} = \sum_{j=1}^{n/2} \frac{bE_c}{1-\upsilon_c^2}\frac{1}{2}\left[z_{c1}^2(j) - z_{c2}^2(j)\right] + \sum_{k=1}^{n/2} \frac{bE_n}{1-\upsilon_n^2}\frac{1}{2}\left[z_{n1}^2(k) - z_{n2}^2(k)\right], \tag{3}$$

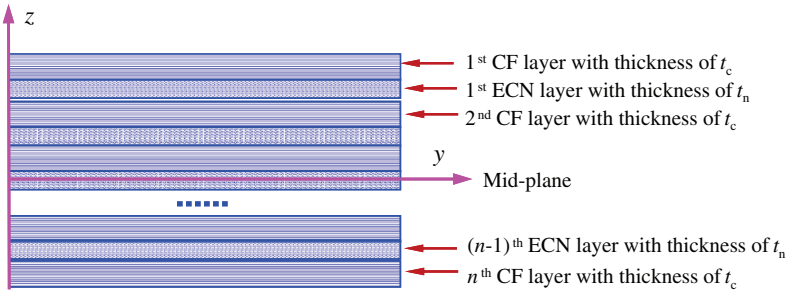

Fig. 5. Schematic diagram of cross-section for a composite laminate with interlaminar regions containing ECN mats. (For interpretation of the references to color in this figure legend, the reader is referred to the web version of this article.)

where ΣEI is the effective flexural rigidity of the entire composite laminate in plane strain, defined as:

$$\Sigma EI = \sum_{j=1}^{n} \frac{bE_c}{1-\upsilon_c^2}\frac{1}{3}[z_{c1}^3(j) - z_{c2}^3(j)] + \sum_{k=1}^{n-1} \frac{bE_n}{1-\upsilon_n^2}\frac{1}{3}[z_{n1}^3(k) - z_{n2}^3(k)], \tag{4}$$

In the above equation, $z_{c1}(j)$ and $z_{c2}(j)$ are the z-coordinates of the upper and lower surfaces of the jth CF fabric layer, respectively; and $z_{n1}(k)$ and $z_{n2}(k)$ are the z-coordinates of upper and lower surfaces of the kth ECN layer of the upper half cross-section, respectively, except for the mid ECN layer with $z_{n2}(n/2) = 0$. Thus, the maximum mid-span deflection of the composite laminate in shear strength test can be determined as:

$$w_{\max} = \frac{P_m L^3}{48(\Sigma EI)}, \tag{5}$$

where L is the span between two pins in the shear strength test. Substitution of Eq. (5) into Eq. (2) leads to the shear strength of composite laminates:

$$\tau_s = 24\frac{Q_{comp} w_{\max}}{bL^3} = \frac{12 w_{\max}}{L^3}\left\{\sum_{j=1}^{n/2} \frac{E_c}{1-\upsilon_c^2}[z_{c1}^2(j) - z_{c2}^2(j)] + \sum_{k=1}^{n/2} \frac{E_n}{1-\upsilon_n^2}[z_{n1}^2(k) - z_{n2}^2(k)]\right\}. \tag{6}$$

Theoretically, relations (2) and (6) are equivalent based on the classic composite beam theory, each of which can be employed for experimental data reduction. However, for either relation (2), (6), one needs to know the effective moduli E_c and E_n and thicknesses t_c and t_n of the CF and ECN mat layers. Considering the possible viscoelastic deformation normally observed in bending tests of polymer composites, relation (2) combined with (4) is preferred, which yields

$$\tau_s = \frac{3P_m}{4b}\frac{\sum_{j=1}^{n/2}\frac{E_c}{1-\upsilon_c^2}[z_{c1}^2(j) - z_{c2}^2(j)] + \sum_{k=1}^{n/2}\frac{E_n}{1-\upsilon_n^2}[z_{n1}^2(k) - z_{n2}^2(k)]}{\sum_{j=1}^{n}\frac{E_c}{1-\upsilon_c^2}[z_{c1}^3(j) - z_{c2}^3(j)] + \sum_{k=1}^{n-1}\frac{E_n}{1-\upsilon_n^2}[z_{n1}^3(k) - z_{n2}^3(k)]}. \tag{7}$$

It can be shown that in the limiting case of isotropic material, relation (7) can recover the case of isotropic materials as shown in relation (1). Furthermore, to examine the applicability of relation (1) in the present study without loss of the generality, only consider an idealized specimen made of two CF fabric layers with thickness h_c and one ECN interlayer with the thickness h_n, and further set $\upsilon_c \approx \upsilon_n$. Thus, relation (7) can be reduced to:

$$\frac{\tau_s}{\frac{3P_m}{4b\times 2(h_c+h_n/2)}} = 1 + \frac{\left(\frac{E_n}{E_c}-1\right)\frac{h_c h_n^2}{2}}{2(h_c+h_n/2)^3 + \left(\frac{E_n}{E_c}-1\right)\frac{h_n^3}{4}}. \tag{8}$$

This relation gives the ratio of the shear strength based on the classic laminate theory (7) to that based on the classic beam theory of isotropic material (1). For ECN reinforced CF-epoxy laminate, if selecting $E_c \approx E_n$, relation (8) shows that relation (1) can give the largely acceptable interlaminar shear strength as expected. For CF-epoxy laminate, if replacing the E_n with the modulus of neat resin E_p ($E_c/E_p > 20$), relation (8) shows that the interlaminar shear strength based on (1) for CF-epoxy laminates is slightly larger than the one given by (7). Therefore, the data acquisition for the studied composite laminates based on the approximate relation (1) does not significantly affect the results and also does not change the conclusions made therein.

4. Concluding remarks

The goal of this study was to develop and evaluate a hybrid multi-scale epoxy composite made of T300® CF fabrics with interlaminar regions containing ECN mats. The hypothesis was that the impregnation of ECNs would substantially improve the out-of-plane properties (*e.g.*, the interlaminar shear strength) of the resulting composite. To test the hypothesis, the (hybrid multi-scale) CF/ECN-epoxy composite and (conventional) CF-epoxy composite were fabricated by the method of VARTM; and their interlaminar shear strength, flexural properties, and electrical conductivities (in both in-plane and out-of-plane directions) were evaluated. The study revealed that the incorporation of ECN mats significantly improved the interlaminar shear strength and flexural properties of the resulting composite. The improvement of interlaminar shear strength was ~86%; the hybrid multi-scale composite also demonstrated appreciable enhancements on out-of-plane and in-plane electrical conductivities, by ~150% and ~20% as compared to the (conventional) CF-epoxy composite. The interfacial reinforcement mechanism was explored by SEM-based fractography. Additionally, a new shear-strength formula was proposed (particularly for the short-beam shear test of composite laminates) by taking into account the effects of ply layup and inter-layers; and a reduced case was analyzed to show the validity of the current study. The developed hybrid multi-scale composite may be used as a replacement of conventional CF/epoxy composite due to its low-cost, low weight penalty, and low impact to the existing composite processing technology.

Acknowledgments

The research conducted at the South Dakota School of Mines and Technology (SDSM&T) was supported by the National Aeronautics and Space Administration (NASA) of the United States (Grant No.: NNX07AT52A) and by the US Air Force Research Laboratory (AFRL) under the Cooperative Agreement Number of

FA9453-06-C-0366. The study conducted at the North Dakota State University (NDSU) was supported by the New Faculty Research Initiative Grant and the NDSU Development Foundation.

References

[1] Mallick PK. Fiber-reinforced composites: materials, manufacturing, and design. New York: Marcel Dekker Inc.; 1993. p. 1–11.
[2] Bkyarova E, Thostenson ET, Yu A, Kim H, Gao J, Tang J, et al. Multiscale carbon nanotube–carbon fiber reinforcement for advanced epoxy composites. Langmuir 2007;23:3970–4.
[3] Zhu J, Imam A, Crane R. Processing a glass fiber reinforced vinyl ester composite with nanotube enhancement of interlaminar shear strength. Compos Sci Technol 2007;67:1509–17.
[4] Thostenson ET, Gangloff JJ, Li CY, Byun JH. Electrical anisotropy in multi-scale nanotube/fiber composites. Appl Phys Lett 2009;97:073111.
[5] Park JK, Do IH, Askeland P. Electrodeposition of exfoliated graphite nanoplatelets onto carbon fibers and properties of their epoxy composites. Compos Sci Technol 2008;68:1734–41.
[6] Ebbesen TW, Lezec HJ, Hiura H. Electrical conductivity of individual carbon nanotubes. Nature 1996;384:147–50.
[7] Allaoui A, Bai S, Cheng HM. Mechanical and electrical properties of a MWNT/epoxy composite. Compos Sci Technol 2002;62:1993–8.
[8] Endo M, Kim YA, Hayashi T. Vapor-grown carbon fibers (VGCFs): basic properties and their battery applications. Carbon 2001;39:1287–9.
[9] Thostenson ET, Li WZ, Wang DZ, Ren ZF, Chou TW. Carbon nanotube/carbon fiber hybrid multiscale composites. J Appl Phys 2002;91:6034–7.
[10] Tsai JL, Wu MP. Organoclay effect on mechanical responses of glass/epoxy nanocomposites. J Compos Mater 2007;41(20):2513–28.
[11] Thostenson ET, Li CY, Chou TW. Nanocomposites in context. Compos Sci Technol 2005:65, 491–516.
[12] Dzenis YA, Reneker DH. Delamination resistant composites prepared by small diameter fiber reinforcement at ply interfaces. US Patent 6265333; 2001.
[13] Dzenis Y. Structural nanocomposites. Science 2008;319:419–20.
[14] Wu XF. Fracture of advanced polymer composites with nanofiber reinforced interfaces. Ph.D. thesis, University of Nebraska-Lincoln; 2003.
[15] Karapapas P, Tsantzalis S, Fiamegou E, Vavouliotis A, Dassios K, Kostopoulos V. Multi-wall carbon nanotubes chemically grafted and physically adsorpted on reinforcing carbon fibers. Adv Compos Lett 2008;17:103–7.
[16] Cipriano BH, Kota AK, Gershon AL. Conductivity enhancement of carbon nanotube and nanofibers-based polymer nanocomposites by melt annealing. Polymer 2008;49:4848–51.
[17] Lee SB, Choi O, Lee W, Yi JW, Kim BS, Byun JH, et al. Processing and characterization of multi-scale hybrid composites reinforced with nanoscale carbon reinforcements and carbon fibers. Compos Part A: Appl Sci Manuf 2011;42:337–44.
[18] Dzenis Y. Spinning continuous fibers for nanotechnology. Science 2004;304:1917–9.
[19] Greiner A, Wendorff JH. Electrospinning: a fascinating method for the preparation of ultrathin fibres. Angew Chem Int Ed 2007;46:5670–703.
[20] Liu J, Yue Z, Fong H. Continuous nano-scaled carbon fibers with superior mechanical strength. Small 2009;5(5):536–42.
[21] Ozden E, Menceloglu YZ, Papila M. Engineering chemistry of electrospun nanofibers and interfaces in nanocomposites for superior mechanical properties. ACS Appl Mater Interf 2010;2:1788–93.
[22] Fong H. Electrospun nylon 6 nanofiber reinforced Bis-GMA/TEGDMA dental restorative composite resins. Polymer 2004;45:2427–32.
[23] Lin S, Cai Q, Ji J, Sui G, Yu Y, Yang X, et al. Electrospun nanofiber reinforced and toughened composites through in situ nano-interface formation. Compos Sci Technol 2008;68:3322–9.
[24] Liu Y, Hedin NE, Fong H. Polycarbonate/poly (methyl methacrylate) nanofiber composites with improved impact strength. J Adv Mater 2008;40(3):33–42.
[25] Li J, Sham ML, Kim JK. Morphology and properties of UV/ozone treated graphite nanoplatelet/epoxy nanocomposites. Compos Sci Technol 2007;67:296–305.
[26] Hibbs MF, Tse MK, Bradley WL. Interlaminar fracture toughness and real-time fracture mechanism of some toughened graphite/epoxy composites. In: Johnston Norman J. editor. Toughened composites, ASTM STP, 937. American Society for Testing and Materials; 1987. p. 115–30.
[27] Mourtiz AP, Gallagher J, Goodwin AA. Flexural strength and interlaminar shear strength of stitched GRP laminates following repeated impacts. Compos Sci Technol 1997;57:509–22.
[28] Chou TW. Microstructural design of fiber composites. UK: Cambridge University Press; 1992.
[29] Barthelot JM. Composite materials: mechanical behavior and structural analysis. New York: Springer; 1997.
[30] Vable M. Intermediate mechanics of materials. UK: Oxford University Press; 2008.